DC Conduction and Dielectric Behavior of (Bi,Pb)-2223 Superconductor when adding Ag Nanoparticles

Mustafa Q. Al-Habeeb
Department of Dentistry, College of Al-Farabi University, Baghdad, Iraq
musttkut@gmail.com (corresponding author)

Fadhil A. Umran
Department of Optics Techniques, College of Al-Farabi University, Baghdad, Iraq
fadhilumran@yahoo.com

Akram N. Mohammed
Department of Optics Techniques, College of Al-Farabi University, Baghdad, Iraq
akram.noori51@gmail.com

Received: 30 November 2024 | Revised: 6 January 2025 | Accepted: 18 January 2025

 DOI: https://doi.org/10.48084/etasr.9780

ABSTRACT

In this paper, the dielectric behavior of $Bi_{1.7}Pb_{0.3}Sr_2Ca_2Cu_3O_{10+\delta}$ ceramic superconductor and the effects of Ag nanoparticle addition were studied at room temperature. The X-ray diffraction pattern reveals that all samples crystallize in orthorhombic structures. The optimal value of critical transition temperature (Tc) was found at addition weight percentage x = 1.2 wt%. The influence Ag nanoparticle adding for changing the Bi-2223 phase's dielectric characteristics were studied along with the determination of the capacitance for ranging frequencies from 50 Hz to 1 MHz. The results show that the dielectric constant decreases with increasing Ag nanoparticle content, indicating the enhancement of the carrier concentration in the CuO_2 planes. The presence of Cu atoms in the CuO_2 and the $Bi_2Sr_2O_{5-\delta}$ charge reservoir layers in (Bi,Pb)-2223 superconductors gives them partially insulating/conducting characteristics, probably improving the doping efficiency of the mobile charge carriers.

Keywords-Ag nanoparticle addition; (Bi,Pb)-2223 superconductors; carriers; dielectric constant

I. INTRODUCTION

The superconducting ceramic compound BSCCO ($Bi_2Sr_2Ca_{n-1}Cu_nO_{2n+4+\delta}$ (n = 1, 2, 3), also termed as (Bi-2201), (Bi-2212), and (Bi-2223)), can be considered as one of the most important and reliable materials in the construction of devises and many scientific practical applications due to its high transition temperature (T_c) and high critical magnetic field. The superconducting compound BSCCO has three different phases of transition temperature: 10, 85, and 110 K, respectively, while n refers to the number of two CuO_2 layers in the unit cell. Bi-2223 is the most interesting phase for many researchers [1]. Significant attempts have been conducted to raise the critical temperature of the superconducting transition, T_c , to room temperatures following the groundbreaking discovery of high-temperature superconductors (HTSC) [2]. The two basic components of the orthorhombic crystal structures of the BSCCO superconductors system are the insulating block layers, which can donate holes or electrons to the Cu layers by acting as electrically active charge repositories, and the essential, superconducting Cu layers or planes [3, 4]. Doping of nanoparticles can be considered an important method for improving the ability to stabilize flow and contact between the grains of the superconducting materials (Bi,Pb)-2223. Recently, much research has been conducted on the impact of nano particle addition, e.g. Au, Ag [2, 4], to enhance superconducting qualities, including metal nanoparticles,e.g. Eu, La, Mg, W, etc. [6-8], nanooxides such as Al_2O_3, MgO, Co_3O_4, $BaFe_{12}O_{19}$, ZrO_2, $BaSnO_3$, MgB_2, and V_2O_5 [9–17], and nano-compounds such as PbS and PbF_2 [1, 18].

Generally, the nanoscale addition to the Bi2223 system may lead to the stabilization and easy settlement of nanoparticles between the particles of the high-temperature superconducting compound, which in turn may lead to the enhancement of the critical current density and flux pinning. According to [3], the addition of Au nanoparticles to (Bi, Pb)-2223 led to modifications in the insulation properties while increasing critical current density (J_c) and transition temperature (T_c).

However,it has been shown that nanoparticles stabilize at grain boundaries without altering the superconductivity of the host structure, and the maximum values of the dielectric characteristics of $(BaFe_{12}O_{19})x$(Bi,Pb)-2223 were found at low frequencies and high temperatures, with improved T_c and J_c.[10, 12]. Frequency-dependent dielectric measurements are very useful for studying the dipolar polarization and the dielectric properties of a material. These studies were done at lower temperatures and helped qualitatively assess the strength of the coupling of charge carriers. Moreover, a medium made up of strongly coupled mobile carriers would be in less polarized condition and have a lower dielectric constant. The dielectric constant determines the nature of the superconducting material, which is dictated by the binding forces that bind the mobile carriers between the conducting $Ag\,O_2$ /$Cu\,O_2$ planes and the $Bi_{1.7}Pb_{0.3}Sr_2Ca_2Cu_3O_{10}$ charge reservoir layers [19, 20].

This work is clearly of the definite interest for improving of functional properties of studied superconducted ceramics due to the fact that the insertion of Ag nanoparticles to (Bi, Pb)-2223 could improve vortex lattice pinning properties, improve communication between grains, and rise *Tc*. The primary factors for choosing the materials of devices for many applications are ac-conductivity, conductance, capacitance, dielectric loss, and dielectric constant. Using C and G measurements of (Ag NPs)$xBi_{1.7}Pb_{0.3}Sr_2Ca_2Cu_3O_{10+\delta}$ in the test frequency (f) range of 50 Hz to 1 MHz, the dielectric parameters (ε_r, ε_i, |tanδ| and σ_{ac}) can be measured as follows:

The dielectric constant real part (ε_r), an indication of the degree to which a material can be polarized can be calculated by [19, 21]:

$$\varepsilon_r = Cd/A\,\varepsilon_0 \quad (1)$$

where d is the thickness of the pellet (m), A is the area of the electrode (m^2), ε_o is the permittivity of free space (8.85×10^{-12} F. m^{-1}), and C is the capacitance (F).

The dielectric constant imaginary part (ε_i) signifies the dielectric loss in the medium (damping factor). Equation (2) can be used to get the material's imaginary portion from the conductance (G):

$$\varepsilon_i = Gd/\omega A\,\varepsilon_0 \quad (2)$$

where $\omega = 2\pi f$, with f being the frequency of the applied ac-field.

The following relation can be used to calculate the dielectric loss (tan δ):

$$\tan\delta = \varepsilon_i/\varepsilon_r \quad (3)$$

AC conductivity, σ_{ac}, is a measure of a material's ability to transport an alternating electrical current:

$$\sigma_{ac} = \omega\varepsilon_0\varepsilon/\tan\delta \quad (4)$$

II. MATERIALS AND METHODS

The polycrystalline bulk $Bi_{1.7}Pb_{0.3}Sr_2Ca_2Cu_3O_{10+\delta}$ ceramic samples with and without the addition of Ag nanoparticles were synthesized by the solid-state reaction method using high purity powders (99.999%) of Bi_2O_3, Pb_3O_4, $Sr(NO_3)_2$, CaO, and CuO proportional to their molecular weights which were used as starting compounds. Ag nanoparticles of 20-30 nm were added by weight percentages x = 0.0, 0.35, 0.6, 0.95 and 1.2 wt%. These compounds were mixed in appropriate ratios by employing a mill machine (SPEX Industries Inc., USA) for 10 min and then manually grinding the powder for another 10 min with an agate mortar and pestle. The mixture was homogenized by adding enough 2-propanol to create a paste while grinding for around 30 min. The mixtures were then calcined in air using a tube furnace set at 810 ˚C for 24 h at a rate of 3 ˚C/min. The mixture was then compressed using a hydraulic press of the SPECAC type at a pressure of 0.7 GPa to form pellets with a diameter of 13 mm and a thickness of 2-3 mm. The pellets were sintered for 144 h at 835 ˚C in a tube furnace. X-Ray Diffraction (XRD) was used to analyze each sample. The dielectric constant was calculated by measuring the capacitance (C) with the aid of an LCR meter analyzer type (GW INSTEK, LCR-8105G) for frequency range (50 Hz- 1 MHz), at Room Temperature (RT).

III. STRUCTURAL PROPERTIES

Figure 1 shows the XRD patterns of the samples with and without the inclusion of Ag nanoparticles.

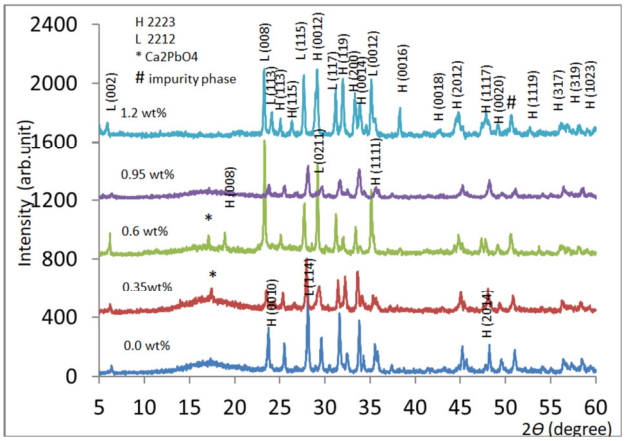

Fig. 1. XRD patterns of (Bi,Pb)-2223 superconducting samples supplemented with Ag nanoparticles.

The XRD pattern deviation results show that all samples have an orthorhombic structure with both phases present (HTS phase Bi-2223 and LTS phase Bi-2212, with HTS being the dominant phase). After adding the Ag nanoparticles, some samples showed weak impurity phases of Ca_2PbO_4 peak at 2θ = 17.34˚ and impurity phase peak at 2θ = 50.58˚. Similar results were obtained in [19, 22]. As a result of the increased concentration of Ag nanopricles, the intensity of several peaks for the Bi-2223 phase increased, starting from (002) at 2θ = 6.18˚∓0.4˚ to (2012) at 2θ = 44.54˚ ∓ 0.3˚ for Bi-2223. This indicates that nano-Ag particles have an effect on grain crystallization and systematic growth under the degree of molecular melting. Moreover, they are linked to the broadening of some peaks as a result of the 2223-phase overlapping with the 2212-phase, as shown in the 0.6 and 1.2 wt% cases. Similar results were obtained in [19, 22] for different compounds.

The calcinations or/and sintering temperature, which are related to the melting temperature, can cause a significant decomposition in oxygen to re-form the Bi-2223 phase, which contains more (Bi,Pb)-rich phases, and cause the peak of Ca_2PbO_4 and impurity phases to emerge from secondary peaks. As seen at 0.6 and 1.2 wt% graphs, these impurity phases have an influence on the volume fraction as well as the lattice properties, particularly the *c*-axis. In order to enhance the structural characteristics of all prepared samples, the c-axis increased (Table I) [4, 5, 24]. The insertion of Ag nanoparticles to (Bi,Pb)-2223 may serve as pinning centers to fix vortices and to improve communication between the grains, potentially raising T_c.

TABLE I. PARAMETERS OF CHARACTERISTIC PHASES OF Agx/(Bi,Pb)-2223 SAMPLES

Ag NPs wt.%	**a** $\overset{o}{A}$	**b** $\overset{o}{A}$	**c** $\overset{o}{A}$	**V** $\overset{o^3}{A}$	$\frac{c}{a}$	ρ_M mg/cm^3	**Volume Fraction** HTC %	LTC %
0.0	5.4124	5.4290	37.0619	1089.04	6.849	1.561	58.61	41.39
0.35	5.4136	5.3674	37.0723	1077.21	6.848	1.578	65.52	34.48
0.6	5.4068	5.3345	37.1189	1070.61	6.865	1.587	62.28	37.72
0.95	5.2206	5.9500	36.9260	1147.02	7.073	1.482	68.64	31.36
1.2	5.4595	5.4002	37.2047	1096.88	6.815	1.549	75.82	24.18

IV. ELECTRICAL RESISTIVITY

The variation of the critical temperature (T_c), i.e. the temperature at which the electrical resistivity of a metal falls to zero, with Ag nanoparticle concentration is shown in Figure2. A metal-like normal condition was revealed by the electrical resistance curves. Figure 2 displays the dc resistivity ρ (Ω cm) against temperature T (K) range $T_0 < T < 300$ K as well as measurements of the nominal composition samples $Bi_{1.7}Pb_{0.3}Sr_2Ca_2Cu_3O_{10+\delta}$without and with nano-Ag addition.

When resistivity against temperature was measured at high temperatures prior to the superconducting transition, all the samples showed metallic behaviors. Interestingly, all the samples with Ag nanoparticles added had higher T_c values than the (Bi,Pb)-2223 (nano-Ag 0.0 0 wt%) sample, with the exception of the (0.6 wt%) sample, probalby due to the infleunce of oxygen content, as is shown in Table II.

The difference between T_c and T_0 is the superconducting transition width (ΔT). A small value of ΔT is considered a measure of the sample's quality or purity since it indicates the presence of percolating pathways that short out the current by first becoming superconducting. By increasing the contact area between the superconducting grains, the widening behavior may be reduced, as in the 0.6 wt% case [19].

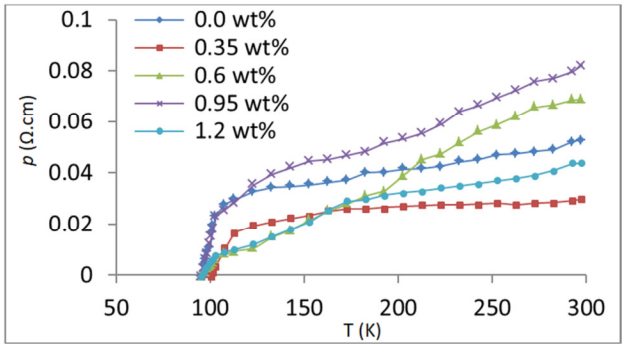

Fig. 2. ρ-T plots for samples of pure and Ag nanoparticle added $Bi_{1.7}Pb_{0.3}Sr_2Ca_2Cu_3O_{10}$.

The improvement of weak linkages between the superconducting grains by the healing of a greater void and pore or superconducting volume fraction with Ag nanoparticles raises T_c. In this instance, Ag-nano samples exhibit T_c and $T_{(c\ R=0)}$ values that rise and then fall at 0.6 wt% addition due to the weak coupling that will result from the random orientation of superconducting crystals and the coexistence of nonsuperconducting impurities, like Ag and Pb ions, at the grain boundaries. This will lower the zero-resistance temperature and broaden the T_c [5, 19]. Thus, the ideal carrier concentration and elevated superconducting volume fraction of the samples as a result of impact oxygen post-sintering are the most likely causing of the improvement in superconductivity (as in 0.35 and 1.2 weight percent parameters) [23, 25]. As demonstrated by the findings derived from the XRD data.

TABLE II. T_C AND ΔT FOR Agx/(Bi,Pb)-2223 SAMPLES

Ag NPs wt.%	T_c **(K)**	$T_{c\,(R=0)}$ **(K)**	ΔT_c **(K)**	**δ**
0.0	110	103	7	0.0437
0.35	113	101	12	0.0689
0.6	108	98	10	0.0575
0.95	110	97	13	0.0477
1.2	113	96	17	0.108

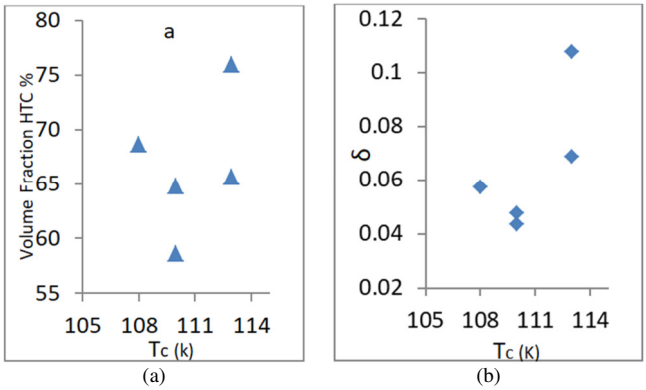

(a) (b)

Fig. 3. Relation between T_c and (a) volume fraction, (b) δ.

Figure 3 shows the relation between T_c and oxygen content (δ) and Volume Fraction of (Bi,Pb)-2223 samples. The optimum nano-Ag concentration for maximum T_c value is seen in the 0.35 and 1.2 wt% samples, the latter also showing maximum oxygen contents (δ) for the samples as shown in Table II.

V. DIELECTIC PROPERTIES

The fluctuations in the dielectric properties of $Bi_{1.7}Pb_{0.3}Sr_2Ca_2Cu_3O_{10+\delta}$ for samples supplemented with Ag nanoparticles were studied as functions of the applied frequency (50 Hz – 1 MHz). The dielectric constants (ε_r and ε_i), loss (tanδ) and ac- conductivity (σ_{ac}) were calculated for each sample with (1)-(4). The amount of energy stored in a material when it is exposed to an electric field is represented by ε_r as a function of frequency for different amounts of added Ag nanoparticles, using (1), as can be seen in Figure 4(a). The intra-granular sites represent the most likely location for this energy to be stored in the material. Generally, the samples demonstrated distinct behaviors at different addition percentages of Ag nanoparticles, and the values of ε_r ranged between 2.584 and 2.189 at the low frequency of 4.77 Hz (Table III). These ε' values are attributed to the interfacial polarization that occurs mainly in the low frequency range. Because the free negative charge carriers (electrons) move from the ceramic sample toward the metal electrodes, the material's composition inside the conducting planes has to be changed, having the carriers there. Electrons can migrate from ceramics to metal surfaces because their Fermi level is greater than that of metals. Moreover, ceramics have fewer filled states than metals, which are most likely causing the shift behavior between before and after the addition. The monitored behavior is in agreement with the results obtained in [19, 21, 25].

The dielectric constant imaginary part ε_i indicates how much energy is absorbed and attenuated across interfaces when an external electric field is applied. Grain boundaries, localized defects, and localized charge concentrations at the defect sites are examples of interfaces. Figure 4(b) shows the change in ε_i versus log$f$ at different additions from Ag nanoparticles of (Bi,Pb)-2223 samples, as listed in Table III. It has been observed that the decreasing in energy attenuation after the addition can be attributed to the increase of oxygen content in the $Bi_{1.7}Pb_{0.3}Sr_2Ca_2Cu_3O_{10+\delta}$ charger reservoir layer. Additionally, since the charge reservoir layer contains localized charges at the Bi^{+3}, Cu^{+2}, and Ag^{+1} sites, the separation of charges between the $Bi_2Sr_2O_{5-\delta}$ charge reservoir layer and mobile carriers in the conducting CuO_2 planes is most likely causing the polarization. Dielectric constant decrease and ε_i increase can be caused by an applied electric field. Similar behavior has been reported in [3, 10, 19].

An explanation for the variation between ε_r and ε_i could be that the double Bi-layer compound has a thicker $Bi_2Sr_2O_{5-\delta}$ charge reservoir layer, which means that when the number of mobile carriers available for dipolar polarization is decreased, the dielectric constant increases the density of carriers in the CuO_2 planes. Since Cu atoms are present, the compound of the (Bi,Pb)-2223 superconductor with the impurity of Pb and Ag nanoparticle additions has partially insulating or conducting characteristics, which probably increase their doping efficiency, as indicated in [17, 19, 21].

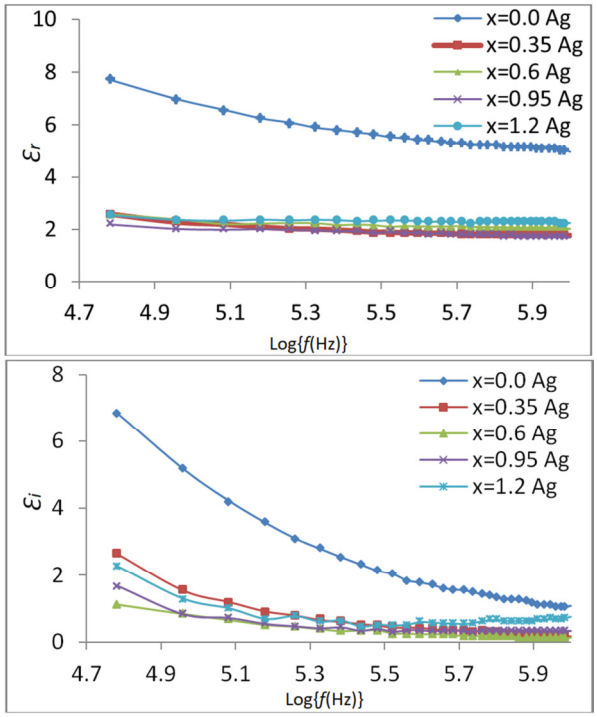

Fig. 4. (a) Dielectric constant real part (ε_r) and (b) Imaginary part of dielectric (ε_i), versus Log f of the external field applied at room temperature on $Bi_{1.7}Pb_{0.3}Sr_2Ca_2Cu_3O_{10+\delta}$ superconductors with various Ag nanoparticles addition.

The dielectric loss factor (|tanδ|) is determined by the ratio of the energy stored in the material to the dissipated energy. All absolute values of samples' of |tanδ| versus Log f are plotted in Figure 5(a). Dielectric loss was considered to determine the mechanism of ac-conduction and dielectric relaxation that may be in the form of leakage currents. Clearly, the presence of Ag nanoparticles boosted these currents, where the value of |tanδ| systematically decreases with decreasing addition of Ag nanoparticles, as shown in Table III.

The ac-conductivity (σ_{ac}) of these samples is shown in Figure 5(b). The maximum value of σ_{ac} at 0.0 wt% addition was around 2.310×10^{-7} and it decreased with increasing addition of Ag nanoparticles as shown in Table III. This adding enhances the efficiency to such an extent that it reaches superconductivity at a very high concentration (1.2 wt %). Moreover, the dielectric constant decreases with increasing addition percentage, which enhanced the carrier concentration in the AgO_2/CuO_2 planes, whereas a decrease in capacitance, ε_r, ε_i, tanδ and σ_{ac} was also observed. The presence of Cu atoms in the CuO_2 and Bi_2CuO_4 charge reservoir layers in (Bi,Pb)-2223 superconductors gives them a partially insulating/conducting character, which probably improves the mobile charge carriers. In other words, the electronegativity of nano-Ag posses has the same effect with that of Cu, whose dielectric is constant and is directly dependent on the polarizibility of the dielectric material, which is directly related

to the electronegativity of the constituent atoms [19, 21, 26]. Therefore, due to the need for smaller and more durable devices, such as memory devices and capacitors, such materials with high dielectric constants are becoming more and more important in the race of microelectronics. Yet cuprates' high conductivity, causes a substantial dissipation loss, which is the primary barrier to their possible use as dielectrics [21].

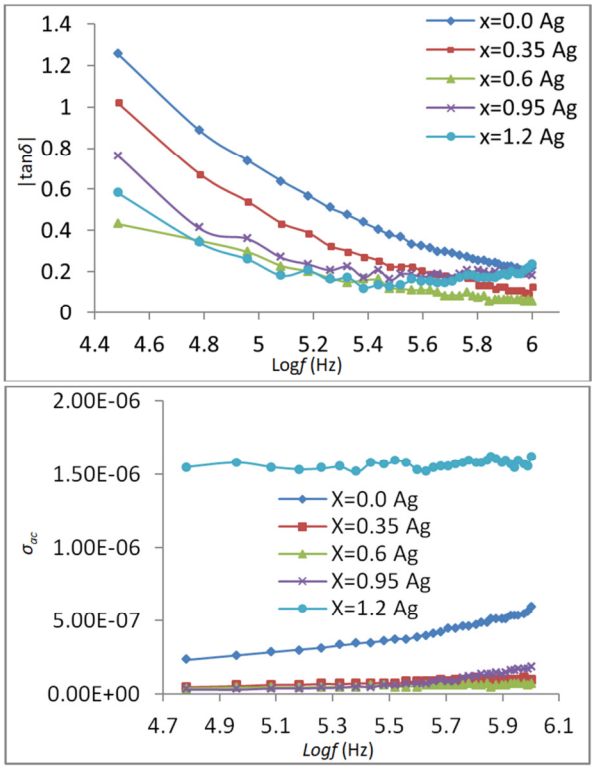

Fig. 5. (a) Absolute value of dielectric loss |tanδ| and (b) ac-conductivity (σ_{ac}) versus Log$f$ of the external field applied at room temperature on $Bi_{1.7}Pb_{0.3}Sr_2Ca_2Cu_3O_{10+\delta}$ superconductors for various Ag nanoparticle addition percentages.

TABLE III. VARIATION OF ε_r, ε_i, TANδ AND σ_{ac} FOR (nano-Ag)x/$Bi_{1.7}Pb_{0.3}Sr_2Ca_2Cu_3O_{10}$

f = 50 Hz- 1MHz				
Ag NPs wt.%	$\boldsymbol{\varepsilon_r}$	$\boldsymbol{\varepsilon_i}$	**tanδ**	$\boldsymbol{\sigma_{ac} \times 10^{-7}}$ $\boldsymbol{(\Omega.m)^{-1}}$
0.0	7.708	6.84	1.259	2.310
0.35	2.536	2.64	1.022	0.446
0.6	2.584	1.116	0.432	0.376
0.95	2.189	1.679	0.767	0.233
1.2	2.368	2.277	0.583	0.146

VI. CONCLUSIONS

The effects of Ag nanoparticles on the superconductivity and dielectric properties of $Bi_{1.7}Pb_{0.3}Sr_2Ca_2Cu_3O_{10}$ superconductor samples were studied in this worl. In the XRD pattern of the (Bi,Pb)-2223 superconductors, it has been observed that there are two weak phases of impurity after the addition of nano-Ag. The weak phase influenced the volume fraction as well as the lattice properties, particularly the c-axis. The magnitude (R = 0) in the samples with added nano-Ag/(Bi,Pb)-2223 is comparatively bigger and exhibits an increase of 113 K at 0.35 and 1.2 wt%, due to the optimal carrier concentration and increased superconducting volume fraction of the samples due to the effect of oxygen post-sintering. The dielectric constants (ε_r and ε_i), loss (tanδ) and ac-conductivity (σ_{ac}) of the prepared samples are significantly influenced by the frequency of the applied ac field, due to the dipolarization caused by the displacement of the mobile electronic charges in the conducting planes from the equilibrium position with respect to the (Bi,Pb)-2223 charge reservoir layer, which is responsible for the dielectric dispersion and the negative capacitance effects. The addition of Ag nanoparticles reduces the carrier density in the conducting planes, with low superconductivity parameters. So, dielectric constants can be applied in capacitors, and the sample with high dielectric constants, (1.2 wt%) is of great importance in electronic applications.

REFERENCES

[1] M. J. Masnita, R. Awang, and R. Abd-Shukor, "AC Susceptibility and Electrical Properties of PbS added $Bi_{1.6}Pb_{0.4}Sr_2CaCu_2O_8$ Superconductor," *Sains Malaysiana*, vol. 51, no. 1, pp. 315–328, Jan. 2022, https://doi.org/10.17576/jsm-2022-5101-26.

[2] J. Chigvinadze, S. Ashinov, G. Mamniashvili, G. Donadze, A. Peikrishvili, and B. Godibadze, "On the Nature of Superconducting Precursors in Bi-Pb-Sr-Ca-Cu-O Compositions Fabricated by Hot Shock Wave Consolidation Technology," *Engineering, Technology & Applied Science Research*, vol. 8, no. 3, pp. 3032–3037, Jun. 2018, https://doi.org/10.48084/etasr.2077.

[3] S. F. Oboudi and M. Q. M. Al-Habeeb, "Dielectric Properties and DC conductivity of Au Nanoparticles Doped Bulk $Bi_{1.7}Pb_{0.3}Sr_2Ca_2Cu_3O_{10+\delta}$ Superconductor", *Iraqi Journal of Science*, Special Issue, Part B, pp. 380-387, Oct. 2016.

[4] A. Jabbar, M. Mumtaz, and K. Nadeem, "Noble metals (Ag, Au) nanoparticles addition effects on superconducting properties of CuTl-1223 phase," *The European Physical Journal Applied Physics*, vol. 69, no. 3, Mar. 2015, Art. no. 30601, https://doi.org/10.1051/epjap/2015140356.

[5] S. F. Oboudi and M. Q. AL-Habeeb, "Gold Nanoparticles Effect on (Bi,Pb)-2223 Superconducting Thin Films," *Applied Physics Research*, vol. 8, no. 5, pp. 64–74, Sep. 2016, https://doi.org/10.5539/apr.v8n5p64.

[6] N. Loudhaief, M. Ben Salem, and M. Zouaoui, "Synthesis and characterization of Eu- and La-doped CuS nanoparticles and their effects on the electrical properties of $(Bi, Pb)_2Sr_2Ca_2Cu_3O_\delta$ superconductor," *Journal of Materials Science: Materials in Electronics*, vol. 32, no. 1, pp. 453–472, Jan. 2021, https://doi.org/10.1007/s10854-020-04793-7.

[7] G. Y. Hermiz, "Dielectric Properties of $Bi_{1.6}Pb_{0.4}Sr_2Ca_{2-x}Mg_xCu_3O_{10+\delta}$ ($0 \leq x \leq 0.5$) Superconducting System", *International Journal of Innovative Research in Science, Engineering and Technology*, vol. 3, no 1, pp. 8564-8572, Jan. 2014.

[8] M. J. Tuama and L. K. Abbas, "Superconducting Properties of $Bi_{2-x}Pb_{0.3}W_xSr_2Ca_2Cu_3O_{10+\delta}$ Compounds," *Iraqi Journal of Science*, vol. 62, no. 2, pp. 490–495, Feb. 2021, https://doi.org/10.24996/ijs.2021.62.2.15.

[9] M. Hernandez-Wolpez *et al.*, "Magnetic relaxation in (Bi,Pb)-2223 superconducting ceramics doped with α-Al_2O_3 nanoparticles," *Revista mexicana de física*, vol. 66, no. 1, pp. 42–46, Feb. 2020, https://doi.org/10.31349/revmexfis.66.42.

[10] A. S. Baqi, N. S. Abed, and S. J. Fathi, "Study the effects of MgO nanoparticle addition on superconducting characteristics of $Bi_{1.6}Ag_{0.4}Sr_{1.9}Ba_{0.1}Ca_2Cu_3O_{10+\delta}$ system," *Journal of Ovonic Research*, vol. 18, no. 2, pp. 273–280, Apr. 2022, https://doi.org/10.15251/JOR.2022.182.273.

[11] A. N. Jannah, R. Abd-Shukor, and H. Abdullah, "Effect of Co_3O_4 Nanoparticles Addition on (Bi,Pb)-2223 Superconductor," *International Journal of Mathematical, Computational, Physical, Electrical and Computer Engineering*, vol. 7, no. 3, pp. 362–365, 2013.

[12] K. Habanjar, F. El Haj Hassan, and R. Awad, "Physical and dielectric properties of (Bi,Pb)-2223 superconducting samples added with $BaFe_{12}O_{19}$ nanoparticles," *Chemical Physics Letters*, vol. 757, Oct. 2020, Art. no. 137880, https://doi.org/10.1016/j.cplett.2020.137880.

[13] M. Zouaoui, A. Ghattas, M. Annabi, F. Ben Azzouz, and M. Ben Salem, "Effect of nano-size ZrO_2 addition on the flux pinning properties of (Bi,Pb)-2223 superconductor," *Superconductor Science and Technology*, vol. 21, 2008, Art. no. 125005, https://doi.org/10.1088/0953-2048/21/12/125005.

[14] M. Me. Barakat and K. Habanjar, "Magnetoresistivity studies for BiPb-2223 phase added by $BaSnO_3$ nanoparticles," *Journal of Advanced Ceramics*, vol. 6, no. 2, pp. 100–109, Jun. 2017, https://doi.org/10.1007/s40145-017-0222-8.

[15] M. S. Shalaby, M. H. Hamed, N. M. Yousif, and H. M. Hashem, "The impact of the addition of Bi_2Te_3 nanoparticles on the structural and the magnetic properties of the Bi-2223 high-Tc superconductor," *Ceramics International*, vol. 47, no. 18, pp. 25236–25248, Sep. 2021, https://doi.org/10.1016/j.ceramint.2021.05.244.

[16] H. Chen, Y. Li, Y. Qi, M. Wang, H. Zou, and X. Zhao, "Critical Current Density and Meissner Effect of Smart Meta-Superconductor MgB_2 and Bi(Pb)SrCaCuO," *Materials*, vol. 15, no. 3, Jan. 2022, Art. no. 972, https://doi.org/10.3390/ma15030972.

[17] S. Cavdar, H. Koralay, and S. Altındal, "Effect of Vanadium Substitution on the Dielectric Properties of Glass Ceramic Bi-2212 Superconductor," *Journal of Low Temperature Physics*, vol. 164, no. 1, pp. 102–114, Jul. 2011, https://doi.org/10.1007/s10909-011-0361-1.

[18] M. Anas, "The effect of PbF_2 doping on the structural, electrical and mechanical properties of (Bi,Pb)–2223 superconductor," *Chemical Physics Letters*, vol. 742, Mar. 2020, Art. no. 137033, https://doi.org/10.1016/j.cplett.2019.137033.

[19] *S. F. Oboudi and M. Q. M. Al-Habeeb, "Dielectric And Transport Properties Of Ag Nanoparticles $Bi_{1.7}Pb_{0.3}Sr_2Ca_2Cu_3O_{10+\delta}$ Added Superconductor Compound," Asian Academic Research Journal of Multidisciplinary, vol. 3, no. 3, pp. 7–18, 2016.*

[20] A. Younis, N. A. Khan, and N. U. Bajwa, "Dielectric Properties of $Cu_{0.5}Tl_{0.5}Ba_2Ca_3Cu_{4-\gamma}Zn_\gamma O_{12-\delta}$ (y = 0, 3) Superconductors," *Journal of the Korean Physical Society*, vol. 57, no. 6, pp. 1437–1443, Dec. 2010, https://doi.org/10.3938/jkps.57.1437.

[21] *M. Mumtaz, N. A. Khan, and S. Khan, "Study of Dielectric Properties of Oxygen-Post annealed $Cu_{0.5}Tl_{0.5}Ba_2Ca_2(Cu_{3-\gamma}M_\gamma)O_{10-\delta}$ Superconductor," IEEE Transactions on Applied Superconductivity*, vol. 23, no. 2, Apr. 2013, Art. no. 8800108, https://doi.org/10.1109/TASC.2013.2245505.

[22] Z. 'Atiqah Mohiju, M. Mujaini, and N. A. Hamid, "Superconducting properties of $(Bi,Pb)_2Sr_2Ca_2Cu_3O_x$ (BSCCO-2223) superconductor ceramics prepared by conventional solid-state reaction and co-precipitation methods," *IOP Conference Series: Materials Science and Engineering*, vol. 1231, 2022, Art. no. 012009, https://doi.org/10.1088/1757-899X/1231/1/012009.

[23] A. R. Ahmed, "Study of the Electrical and Structural/Micro structural Properties of $Bi_{2-x}Ag_xBa_{2-y}Sr_yCa_2Cu_3O_{10+\delta}$ System", *Advances in Physics Theories and Applications*, Vol. 39, pp. 33-42, 2015.

[24] O. Ozturk, T. Kucukomeroglu, and C. Terzioglu, "Calculation of the diffusion coefficient of Au in Bi-2223 superconductors," *Journal of Physics: Condensed Matter*, vol. 19, no. 34, 2007, Art. no. 346205, https://doi.org/10.1088/0953-8984/19/34/346205.

[25] A. Abou-Aly, I. Ibrahim, N. Mohammed, and M. Rekaby, "Dielectric properties of $Cu_{0.5}Tl_{0.5}Ba_2Ca_2Cu_3O_{10-\delta}$ superconductor added with nano - Fe_2O_3," *BAU Journal - Science and Technology*, vol. 1, no. 2, Jun. 2020, Art. no. 8, https://doi.org/10.54729/2959-331X.1022.

[26] S. Boumous, S. Belkhiat, and F. Kharchouche, "MgO Effect on the Dielectric Properties of $BaTiO_3$," *Engineering, Technology & Applied Science Research*, vol. 9, no. 3, pp. 4092–4099, Jun. 2019, https://doi.org/10.48084/etasr.2705.